Dirac and Pauli form factors of nucleons using nonlocal chiral effective Lagrangian *

Fangcheng He(何方成)[1,2;1)] Ping Wang(王平)[1,3;2)]

[1] Institute of High Energy Physics, Beijing 100049, China
[2] University of Chinese Academy of Sciences, Beijing 100049, China
[3] Theoretical Physics Center for Science Facilities (TPCSF), Chinese Academy of Sciences, Beijing 100049, China

Abstract: Dirac and Pauli form factors are investigated in the relativistic chiral effective Lagrangian. The octet and decuplet intermediate states are included in the one-loop calculation. The 4-dimensional regulator is introduced to deal with the divergence. Different from the non-relativistic case, this 4-dimensional regulator is generated from the nonlocal Lagrangian with the gauge link, which guarantees local gauge invariance. As a result, additional diagrams appear which ensure electric charge 1 and 0 for proton and neutron respectively. The obtained Dirac and Pauli form factors of the nucleons are all reasonable up to relatively large Q^2.

Keywords: chiral effective lagrangian, nonlocal lagrangian, form factors

PACS: 13.40.Gp, 21.10.Gv, 21.45.Bc **DOI:** 10.1088/1674-1137/41/11/114106

1 Introduction

The study of the electromagnetic properties of the nucleons is very important to help us understand hadron structure. Though QCD is the fundamental theory which describes the strong interaction, it is difficult to study hadron structure using QCD directly due to its nonperturbative behavior. A lot of phenomenological models, such as the cloudy bag model [1], the constituent quark model [2, 3], the $1/N_c$ expansion approach [4], the perturbative chiral quark model [5], the extended vector meson dominance model [6], the $SU(3)$ chiral quark model [7], the quark-diquark model [8, 9], etc., have been proposed. They are widely applied in the calculation of hadron properties, including electromagnetic quantities.

As well as the above model calculations, there are also many lattice simulations on the electromagnetic form factors [10–16]. Though lattice QCD is the most rigorous approach, most quantities are simulated with large quark (π) mass because of computing limitations.

Chiral perturbation theory (χPT) is another useful method to study low-energy physics. Both relativistic and heavy baryon chiral effective field theory have been applied to study the nucleon electromagnetic form factors [17–20]. The results from χPT with dimensional regularization show that it can only describe the form factors at very low Q^2, say $Q^2 < 0.1$ GeV^2 [18]. When the contributions of vector mesons are included, the results are close to those of experiments with $Q^2 < 0.4$ GeV^2 [20].

Another effective way to deal with the divergence of the loop integral is finite-range-regularization (FRR). This has been widely applied to calculate the baryon mass, electromagnetic form factors, strange form factors, charge radii, first moments, proton spin, etc [21–35]. Various investigations show that FRR can be successfully applied to study hadron structure at relatively large pion mass and momentum transfer.

Currently, FRR can only be applied with heavy baryon χPT. In the relativistic case, if we add the covariant/relativistic regulator as in FRR, charge conservation will be destroyed. Therefore, we need to start from a nonlocal gauge invariant Lagrangian to derive the regulator. The advantage of the nonlocal Lagrangian is that it can automatically generate the regulator. The local gauge invariant Lagrangian can be constructed from the gauge link. With this nonlocal Lagrangian, the Ward identity and charge conservation are satisfied. For example, with wave function renormalisation, the proton charge is 1. The neutron charge and the strange charge of the nucleons are also zero. These cannot be obtained with the covariant regulator in the local Lagrangian.

Therefore, in this paper, we will provide a relativistic version of FRR and apply it to the investigation of the Dirac and Pauli form factors of the nucleons. The paper is organized as follows. In Section 2, we briefly in-

Received 15 May 2017, Revised 21 August 2017

∗ Supported by National Natural Science Foundation of China (11475186) and Sino-German CRC 110 (NSFC 11621131001)

1) E-mail: hefc@ihep.ac.cn

2) E-mail: pwang4@ihep.ac.cn

troduce the chiral Lagrangian and nonlocal Lagrangian. The Dirac and Pauli form factors of the nucleons are derived in Section 3. Numerical results are presented in Section 4. Finally, Section 5 gives a summary.

2 Chiral effective lagrangian

The lowest order chiral Lagrangian for the interaction of octet baryons B and decuplets T with pseudoscalar fields ϕ can be written as [36, 37]:

$$\begin{aligned}\mathcal{L}=&DTr\bar{B}\gamma_\mu\gamma_5\{A_\mu,B\}+F\mathrm{Tr}\bar{B}\gamma_\mu\gamma_5[A_\mu,B]\\&+i\mathrm{Tr}\bar{B}\not{D}B-m_B\mathrm{Tr}\bar{B}B+\frac{f^2}{4}Tr\partial_\mu\Sigma\partial^\mu\Sigma^+\\&+\frac{C}{f}\epsilon^{abc}\bar{T}^{ade}_\mu(g^{\mu\nu}+z\gamma_\mu\gamma_\nu)B^e_c\partial_\nu\phi^d_b+\mathrm{H.C},\end{aligned}\tag{1}$$

where D, F and $\mathcal{C}$ are the coupling constants. The chiral covariant derivative D_μ is written as $D_\mu B=\partial_\mu B+[V_\mu,B]$. The pseudoscalar meson octet couples to the baryon field through the vector and axial vector combinations

$$V_\mu=\frac{1}{2}(\zeta\partial_\mu\zeta^\dagger+\zeta^\dagger\partial_\mu\zeta),\qquad A_\mu=\frac{i}{2}(\zeta\partial_\mu\zeta^\dagger-\zeta^\dagger\partial_\mu\zeta),\tag{2}$$

where

$$\zeta=\mathrm{e}^{\mathrm{i}\phi/f},\qquad f=93\ \mathrm{MeV}.\tag{3}$$

The matrix of pseudoscalar fields ϕ is expressed as

$$\phi=\frac{1}{\sqrt{2}}\begin{pmatrix}\frac{1}{\sqrt{2}}\pi^0+\frac{1}{\sqrt{6}}\eta & \pi^+ & K^+\\ \pi^- & -\frac{1}{\sqrt{2}}\pi^0+\frac{1}{\sqrt{6}}\eta & K^0\\ K^- & \bar{K}^0 & -\frac{2}{\sqrt{6}}\eta\end{pmatrix}.\tag{4}$$

The explicit form of the baryon octet is written as

$$B=\begin{pmatrix}\frac{1}{\sqrt{2}}\Sigma^0+\frac{1}{\sqrt{6}}\Lambda & \Sigma^+ & p\\ \Sigma^- & -\frac{1}{\sqrt{2}}\Sigma^0+\frac{1}{\sqrt{6}}\Lambda & n\\ \Xi^- & \Xi^0 & -\frac{2}{\sqrt{6}}\Lambda\end{pmatrix}.\tag{5}$$

In the $SU(3)$ chiral limit, the octet baryons will have the same mass m_B. In our calculation, we use the physical masses for baryon octets and decuplets. The leading order electromagnetic interaction can be obtained by minimal substitution as

$$\begin{aligned}&V_\mu\to V_\mu+\frac{1}{2}ie\mathscr{A}^\mu(\zeta^+Q\zeta+\zeta Q\zeta^+),\\&A_\mu\to A_\mu-\frac{1}{2}e\mathscr{A}^\mu(\zeta Q\zeta^+-\zeta^+Q\zeta),\\&\partial_\mu\Sigma\to\partial_\mu\Sigma+ie\mathscr{A}_\mu[Q,\Sigma].\end{aligned}\tag{6}$$

For baryon decuplets, the covariant Lagrangian is

$$\mathcal{L}=\bar{T}^{abc}_\mu(i\gamma^{\mu\nu\alpha}D_\alpha-m_T\gamma^{\mu\nu})T^{abc}_\nu.\tag{7}$$

M_T is the decuplet mass in the chiral limit. $D_\nu T^{abc}_\mu=\partial_\nu T^{abc}_\mu+(\Gamma_\nu,T_\mu)^{abc}$, where Γ_ν is the chiral connection defined by $(X,T_\mu)=(X)^a_dT^{dbc}_\mu+(X)^b_dT^{adc}_\mu+(X)^c_dT^{abd}_\mu$ [38]. $\gamma^{\mu\nu\alpha}$ and $\gamma^{\mu\nu}$ are the antisymmetric gamma matrices, expressed as

$$\gamma^{\mu\nu}=\frac{1}{2}[\gamma^\mu,\gamma^\nu]\quad\text{ and }\quad\gamma^{\mu\nu\rho}=\frac{1}{4}\{[\gamma^\mu,\gamma^\nu],\gamma^\rho\}.\tag{8}$$

For the baryon decuplets, there are three indices defined as

$$\begin{aligned}&T_{111}=\Delta^{++},\ T_{112}=\frac{1}{\sqrt{3}}\Delta^+,\ T_{122}=\frac{1}{\sqrt{3}}\Delta^0,\\&T_{222}=\Delta^-,\ T_{113}=\frac{1}{\sqrt{3}}\Sigma^{*,+},\ T_{123}=\frac{1}{\sqrt{6}}\Sigma^{*,0},\\&T_{223}=\frac{1}{\sqrt{3}}\Sigma^{*,-},\ T_{133}=\frac{1}{\sqrt{3}}\Xi^{*,0},\ T_{233}=\frac{1}{\sqrt{3}}\Xi^{*,-},\\&T_{333}=\Omega^-.\end{aligned}\tag{9}$$

The octet, decuplet and octet-decuplet transition magnetic operators, which are the next-to-leading-order electromagnetic interaction, are needed in the one-loop calculation of nucleon Dirac and Pauli form factors. The baryon octet magnetic Lagrangian is written as

$$\mathcal{L}=\frac{e}{4m_N}\left(c_1\mathrm{Tr}\bar{B}\sigma^{\mu\nu}\left\{F^+_{\mu\nu},B\right\}+c_2\mathrm{Tr}\bar{B}\sigma^{\mu\nu}\left[F^+_{\mu\nu},B\right]\right),\tag{10}$$

where

$$F^+_{\mu\nu}=-\frac{1}{2}\left(\zeta^\dagger F_{\mu\nu}Q\zeta+\zeta F_{\mu\nu}Q\zeta^\dagger\right).\tag{11}$$

Q is the charge matrix $Q=\mathrm{diag}\{2/3,-1/3,-1/3\}$. At the lowest order, the Lagrangian will generate the following nucleon anomalous magnetic moments as

$$F_2^p=\frac{1}{3}c_1+c_2,\qquad F_2^n=-\frac{2}{3}c_1.\tag{12}$$

The effective decuplet magnetic operator is expressed as [39]

$$\mathcal{L}=-\frac{eg_d}{4m_T}\bar{T}^{abc}_\mu\sigma^{\rho\sigma}g^{\mu\nu}(F^+_{\rho\sigma},T_\nu)^{abc}\tag{13}$$

with $g_d=3.88$.

The transition magnetic operator is [40]

$$\mathcal{L}=\frac{-3ieg_m}{\sqrt{2}m(m+m_T)}\bar{B}^{ab}\epsilon^{cda}Q^{ce}(\partial_\mu T_\nu)^{dbe}\epsilon^{\mu\nu\alpha\beta}\partial_\alpha\mathscr{A}_\beta\tag{14}$$

with $g_M=3.16$.

Finite-range-regularization has previously been applied to deal with divergence in the loop integral in heavy baryon χPT [23, 41]. Physically, this regularization method reflects the size effect of the baryons and mesons. In the relativistic case, as we explained in the Introduction, we need to introduce a nonlocal gauge invariant Lagrangian to derive the covariant regulator. Taking the size effect of the hadrons into account, the interaction between baryons and mesons or between baryons and photons will be nonlocal. We can use the gauge link to generate the gauge invariant non-local Lagrangian. This

method has been used in Refs. [42, 43]. For instance, the local interaction including a π meson can be written as

$$\mathcal{L}_{\pi}^{\rm local}=\int {\rm d}x\frac{D+F}{\sqrt{2}f}\bar{p}(x)\gamma^{\mu}\gamma_5 n(x)(\partial_{\mu}+{\rm i}e\mathscr{A}_{\mu}(x))\pi^{+}(x). \tag{15}$$

The nonlocal Lagrangian for this interaction is expressed as

$$\begin{aligned}\mathcal{L}_{\pi}^{nl}=&\int {\rm d}x\int {\rm d}y\frac{D+F}{\sqrt{2}f}\bar{p}(x)\gamma^{\mu}\gamma_5 n(x)F(x-y)\\&\times\exp[{\rm i}e\int_x^y {\rm d}z_{\nu}\int {\rm d}a\mathscr{A}^{\nu}(z-a)F(a)]\\&\times(\partial_{\mu}+{\rm i}e\int {\rm d}a\mathscr{A}_{\mu}(y-a))F(a))\pi^{+}(y),\end{aligned} \tag{16}$$

where $F(x)$ is the correlation function. With the same idea, the nonlocal electromagnetic interaction can also be obtained. For example, the local interaction between proton and photon is written as

$$\begin{aligned}\mathcal{L}_{EM}^{\rm local}=&-e\bar{p}(x)\gamma^{\mu}p(x)\mathscr{A}_{\mu}(x)\\&+\frac{(c_1+3c_2)e}{12m_N}\bar{p}(x)\sigma^{\mu\nu}p(x)F_{\mu\nu}(x).\end{aligned} \tag{17}$$

The corresponding nonlocal Lagrangian is expressed as

$$\begin{aligned}\mathcal{L}_{EM}^{nl}=&-e\int {\rm d}a\bar{p}(x)\gamma^{\mu}p(x)\mathscr{A}_{\mu}(x-a)F(a)\\&+\frac{(c_1+3c_2)e}{12m_N}\int {\rm d}a\bar{p}(x)\sigma^{\mu\nu}p(x)F_{\mu\nu}(x-a)F(a).\end{aligned} \tag{18}$$

The above nonlocal electromagnetic interaction will generate Q^2 dependent form factors at tree level. The nonlocal Lagrangian is invariant under the following gauge transformation

$$\begin{aligned}&\pi^{+}(y)\to{\rm e}^{{\rm i}\alpha(y)}\pi^{+}(y),\quad p(x)\to{\rm e}^{{\rm i}\alpha(x)}p(x),\\&\mathscr{A}_{\mu}(x)\to\mathscr{A}_{\mu}(x)-\frac{1}{e}\partial_{\mu}\alpha'(x),\end{aligned} \tag{19}$$

where $\alpha(x)=\int {\rm d}a\alpha'(x-a)F(a)$. From the expansion of the nonlocal Lagrangian, one can get the following interaction including one photon

$$\begin{aligned}\mathcal{L}^{nor}=&\int {\rm d}x\int {\rm d}y\frac{D+F}{\sqrt{2}f}\bar{p}(x)\gamma^{\mu}\gamma_5 n(x)F(x-y)\\&\times{\rm i}e\pi^{+}(y)\int {\rm d}a\mathscr{A}_{\mu}(y-a)F(a),\end{aligned} \tag{20}$$

$$\begin{aligned}\mathcal{L}^{add}=&\int {\rm d}x\int {\rm d}y\frac{D+F}{\sqrt{2}f}\bar{p}(x)\gamma^{\mu}\gamma_5 n(x)F(x-y)\\&\times{\rm i}e\int_x^y {\rm d}z_{\nu}\int {\rm d}a\mathscr{A}^{\nu}(z-a)F(a)\partial_{\mu}\pi^{+}(y).\end{aligned} \tag{21}$$

The first Lagrangian is the normal interaction with a photon, and is the same as in the local case. The second Lagrangian is the additional term, which is essential to ensure the renormalized charge of the proton (neutron) is 1 (0). With the obtained nonlocal Lagrangian, we can calculate the Dirac and Pauli form factors.

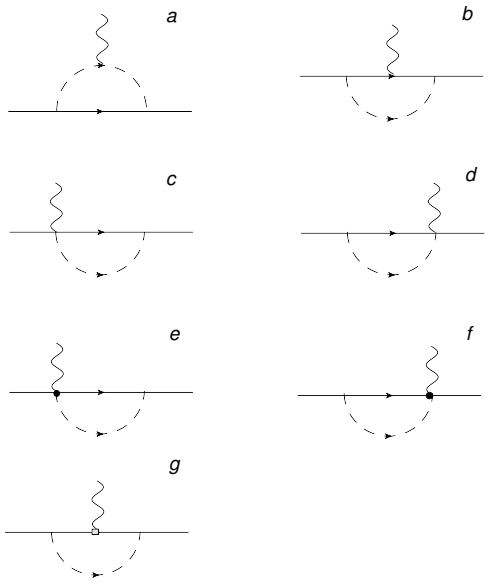

Fig. 1. One-loop Feynman diagrams for nucleon form factors. The solid, dashed and wavy lines are for the baryons, pseudoscalar mesons and photons, respectively. The rectangles and black dots represent magnetic and additional interactions with the photon.

3 Dirac and Pauli form factors

The form factors of the nucleons are defined as

$$\begin{aligned}<N(p')|J^{\mu}|N(p)>=&\bar{u}(p')\{\gamma^{\mu}F_1^N(Q^2)\\&+\frac{{\rm i}\sigma^{\mu\nu}q_{\nu}}{2m_N}F_2^N(Q^2)\}u(p),\end{aligned} \tag{22}$$

where $q=p'-p$ and $Q^2=-q^2$. $F_1^N(Q^2)$ and $F_2^N(Q^2)$ are the Dirac and Pauli form factors. According to the Lagrangian in Eq. (18), the tree level form factors of the proton are expressed as

$$F_1^p(Q^2)=\tilde{F}(Q^2),\quad F_2^p(Q^2)=\frac{c_1+3c_2}{3}\tilde{F}(Q^2), \tag{23}$$

where the function $\tilde{F}(k^2)$ is the Fourier transformation of the correlation function $F(a)$. In the numerical calculation, it is chosen to be a dipole form

$$\tilde{F}(k^2)=\frac{1}{(1-k^2/\Lambda^2)^2}. \tag{24}$$

Similarly, the neutron form factors at tree level are expressed as

$$F_1^n(Q^2)=0,\quad F_2^n(Q^2)=-\frac{2c_1}{3}\tilde{F}(Q^2). \tag{25}$$

The above tree level contribution is very important to get the final results. The momentum dependence of the

tree level form factors provides more curvature than the loop contribution.

The one-loop Feynman diagrams which contribute to the nucleon form factors are plotted in Fig. 1. In our calculation, both octet and decuplet intermediate states are included. Because the expressions for the decuplet part are much more complicated, we will only show the expressions for the octet part.

This updated relativistic version of FRR is also needed for the study of hadron structure at relatively large Q^2, especially for the calculation of parton distribution functions where the formalism is relativistic. A lot of investigations of FRR have been done and we have good knowledge of the non-relativistic regulator, which was kept the same for all the above calculations. However, we know little about the relativistic regulator and this is the first try to determine the relativistic regulator from the well-known form factors of the nucleons. In FRR, there is no cut-off for the k_0 integral in the loop calculation. The regulator is in 3-dimensional $\vec{k}$ space. This non-relativistic regulator is only applied in the heavy baryon chiral effective model calculation. As a result, there are no Kroll-Ruderman or additional diagrams from the gauge link, i.e. Fig. 1(c), 1(d), 1(e) and 1(f) do not appear in that case. In addition, the regulator in the FRR is added when doing the loop integral. There is no momentum dependence of the form factors at tree level. When extrapolating the lattice data, the extrapolation has to be done separately at different Q^2. In other words, the low energy constants are Q^2 dependent, as shown in Table I and II of Ref. [23]. This Q^2 dependence was obtained from fitting lattice data at different momentum transfers. Here, the regulator and the momentum dependence of form factors at tree level is derived from the nonlocal Lagrangian. This make it possible to get the correct momentum dependence of form factors with only one free parameter in the correlation function.

For the octet intermediate states, the contributions of Fig.1(a) are expressed as

$$\Gamma_a^{\mu(p)}=-\frac{(D+F)^2}{2f^2}I_{a\pi}^{NN}-\frac{(3F+D)^2}{12f^2}I_{aK}^{N\Lambda}-\frac{(D-F)^2}{4f^2}I_{aK}^{N\Sigma}, \tag{26}$$

$$\Gamma_a^{\mu(n)}=\frac{(D+F)^2}{2f^2}I_{a\pi}^{NN}-\frac{(D-F)^2}{2f^2}I_{aK}^{NN}. \tag{27}$$

We will only show the expression of the above integrals for the intermediate nucleon state as an example. The loop integral $I_{a\pi}^{NN}$ is expressed as

$$I_{a\pi}^{NN}=\bar{u}(p')\int\frac{\mathrm{d}^4k}{(2\pi)^4}(\not{k}+\not{q})\gamma_5\tilde{F}(q+k)\frac{\mathrm{i}}{D_\pi(k+q)}\times\frac{\mathrm{i}e}{D_\pi(k)}\frac{(2k+q)^\mu}{\not{p}-\not{k}-m_N}(\not{k}\gamma_5)\tilde{F}(k)u(p), \tag{28}$$

where $D_\pi(k)$ is expressed as

$$D_\pi(k)=k^2-M_\pi^2+i\epsilon. \tag{29}$$

Using FeynCalc to simplify the γ matrix algebra and Feynman parameters, we can get the separate expressions for the Dirac and Pauli form factors. The contribution of Fig. 1(b) is expressed as

$$\Gamma_b^{\mu(p)}=\frac{1}{4f^2}(D+F)^2I_{c\pi}^{NN}+\frac{(3F-D)^2}{12f^2}I_{c\eta}^{NN}+\frac{(D-F)^2}{2f^2}I_{cK}^{N\Sigma}, \tag{30}$$

$$\Gamma_b^{\mu(n)}=\frac{(D+F)^2}{2f^2}I_{c\pi}^{NN}-\frac{(D-F)^2}{2f^2}I_{cK}^{N\Sigma}, \tag{31}$$

where

$$I_{b\pi}^{NN}=\bar{u}(p')\tilde{F}(q)\int\frac{\mathrm{d}^4k}{(2\pi)^4}\not{k}\gamma_5\tilde{F}(k)\frac{\mathrm{i}}{D_\pi(k)}\frac{\mathrm{i}}{\not{p}'-\not{k}-m_N}\times(-\mathrm{i}e\gamma_\mu)\frac{\mathrm{i}}{\not{p}-\not{k}-m_N}(-\not{k}\gamma_5)\tilde{F}(k)u(p). \tag{32}$$

The contribution from Fig. 1(c)+1(d) can be written as

$$\Gamma_{c+d}^{\mu(p)}=\frac{-(D+F)^2}{2f^2}I_{(c+d)\pi}^{NN}-\frac{(3F+D)^2}{12f^2}I_{(c+d)K}^{N\Lambda}-\frac{(D-F)^2}{4f^2}I_{(c+d)K}^{N\Sigma}, \tag{33}$$

$$\Gamma_{c+d}^{\mu(n)}=\frac{(D+F)^2}{2f^2}I_{(c+d)\pi}^{NN}-\frac{(D-F)^2}{2f^2}I_{(c+d)K}^{NN}, \tag{34}$$

where

$$I_{(c+d)\pi}^{NN}=\bar{u}(p')\tilde{F}(q)\int\frac{\mathrm{d}^4k}{(2\pi)^4}\not{k}\gamma_5\tilde{F}(k)\frac{\mathrm{i}}{\not{p}'-\not{k}-m_N}\frac{\mathrm{i}}{D_\pi(k)}\times(-e\gamma^\mu\gamma_5)\tilde{F}(q-k)u(p)+\bar{u}(p')\tilde{F}(q)\int\frac{\mathrm{d}^4k}{(2\pi)^4}e\gamma^\mu\gamma_5\tilde{F}(q+k)\times\frac{\mathrm{i}}{\not{p}-\not{k}-m_N}\frac{\mathrm{i}}{D_\pi(k)}(-\not{k}\gamma_5)\tilde{F}(k)u(p). \tag{35}$$

The separate expressions for F_1 and F_2 are expressed as

$$F_{1c+d}^{np}(Q^2)=\frac{(D+F)^2}{f^2}\Lambda^8\tilde{F}(q)\left[\int_0^1\mathrm{d}x_1\mathrm{d}x_4\frac{x_4(x_1+x_4-1)}{8\pi^2\Delta_2^3}+\int_0^1\mathrm{d}x_1\mathrm{d}x_3\mathrm{d}x_4\frac{3x_3x_4(-x_4q^2-x_1m_N^2+mx_1m_N+M_\pi^2)}{8\pi^2\Delta_1^4}\right], \tag{36}$$

$$F_{2c+d}^{np}(Q^2)=\frac{(D+F)^2}{f^2}\Lambda^8\tilde{F}(q)\int_0^1\mathrm{d}x_1\mathrm{d}x_3\mathrm{d}x_4\frac{3x_4^2x_3m_N(m_N+m)}{4\pi^2\Delta_1^4}, \tag{37}$$

where

$$\Delta_1 = (x_1^2-x_1)m_N^2+(x_4^2-x_4)q^2+x_1x_4q^2+m^2x_1 +M_\pi^2(1-x_1-x_3-x_4)+\Lambda^2(x_3+x_4)$$

and

$$\Delta_2=x_4(x_1+x_4-1)q^2+x_1(m^2-m_N^2)+x_1^2m_N^2+\Lambda^2(1-x_1).$$

The expressions of F_1^N and F_2^N for the other diagrams are tedious. Here we only show this simplest F_1 and F_2 as an example. The contribution of Fig. 1(e)+1(f) can be written as

$$\Gamma_{e+f}^{\mu(p)}=\frac{-(D+F)^2}{2f^2}I_{(e+f)\pi}^{NN}-\frac{(3F+D)^2}{12f^2}I_{(e+f)K}^{N\Lambda} -\frac{(D-F)^2}{4f^2}I_{(e+f)K}^{N\Sigma}, \tag{38}$$

$$\Gamma_{e+f}^{\mu(n)}=\frac{(D+F)^2}{2f^2}I_{(e+f)\pi}^{NN}-\frac{(D-F)^2}{2f^2}I_{(e+f)K}^{NN}, \tag{39}$$

where the loop integral is written as

$$\begin{aligned}I_{(e+f)\pi}^{NN}=&\tilde{F}(q)\bar{u}(p')\int\frac{\mathrm{d}^4k}{(2\pi)^4}\not{k}\gamma_5\tilde{F}(k)\frac{\mathrm{i}}{\not{p}'-\not{k}-m_N}\frac{\mathrm{i}e}{D_\pi(k)}\\ &\times\not{k}\gamma_5\frac{(-2k+q)^\mu}{-2kq+q^2}[\tilde{F}(k-q)-\tilde{F}(k)]u(p)\\ &+\tilde{F}(q)\bar{u}(p')\int\frac{\mathrm{d}^4k}{(2\pi)^4}e\not{k}\gamma_5\frac{\mathrm{i}}{\not{p}-\not{k}-m_N}\frac{\mathrm{i}}{D_\pi(k)}\\ &\times(-\not{k}\gamma_5)\tilde{F}(k)\frac{(2k+q)^\mu}{2kq+q^2}[\tilde{F}(k+q)-\tilde{F}(k)]u(p).\end{aligned} \tag{40}$$

The contribution from Fig. 1(g) is expressed as

$$\Gamma_g^{\mu(p)}=\frac{(c_2-c_1)(D+F)^2}{4f^2}I_{g\pi}^{NN}+(\frac{1}{3}c_1+c_2)\frac{(3F-D)^2}{12f^2}I_{g\eta}^{NN} -\frac{(3F+D)^2c_1}{36f^2}I_{gK}^{N\Lambda}+\frac{(D-F)^2(c_1+2c_2)}{4f^2}I_{gK}^{N\Sigma} -\frac{(D-F)(3F+D)c_1}{6f^2}I_{gK}^{N\Lambda\Sigma}, \tag{41}$$

$$\Gamma_g^{\mu(n)}=\frac{c_2(D+F)^2}{2f^2}I_{g\pi}^{NN}-\frac{c_1(3F-D)^2}{18f^2}I_{g\eta}^{NN} -\frac{(3F+D)^2c_1}{36f^2}I_{gK}^{N\Lambda}+\frac{(D-F)^2(c_1-2c_2)}{4f^2}I_{gK}^{N\Sigma} +\frac{(D-F)(3F+D)c_1}{6f^2}I_{gK}^{N\Lambda\Sigma}, \tag{42}$$

where the loop integral is expressed as

$$\begin{aligned}I_{g\pi}^{NN}=&\bar{u}(p')\tilde{F}(q)\int\frac{\mathrm{d}^4k}{(2\pi)^4}\not{k}\gamma_5\tilde{F}(k)\frac{\mathrm{i}}{\not{p}'-\not{k}-m_N}\\ &\times\frac{-e\sigma^{\mu\nu}q_\nu}{2m_N}\frac{\mathrm{i}}{\not{p}-\not{k}-m_N}\frac{\mathrm{i}}{D_\pi(k)}\not{k}\gamma_5\tilde{F}(k)u(p).\end{aligned} \tag{43}$$

With the obtained formulas we can do the numerical calculations, and the results are shown in the next section.

4 Numerical results

In the numerical calculations, the coupling constants are chosen as $D=0.76$ and $F=0.50$ ($g_A=D+F=1.26$). The constant $\mathcal{C}$ is chosen to be 1, which is the same as in Ref. [39]. The low energy constants c_1 and c_2 are determined by $F_2^p(0)=1.79$ and $F_2^n(0)=-1.91$. There is only one free parameter Λ, which is in the dipole regulator. It is found that when Λ is around 0.8 GeV, we can get reasonable results for both proton and neutron form factors.

The proton Dirac form factor $F_1^p(Q^2)$ versus Q^2 is plotted in Fig. 2. The solid line is the empirical result, which is obtained from the combination of the empirical value of $G_E^p(Q^2)=1/(1+\frac{Q^2}{0.71})^2$ and $G_M^p(Q^2)=2.79/(1+\frac{Q^2}{0.71})^2$. The three dashed lines, from bottom to top, represent the results with Λ=0.7 GeV, 0.8 GeV and 0.9 GeV, respectively. As a comparison, the result with dimensional regularization is also shown, by the dotted line. From the figure, one can see at $Q^2=0$, F_{1p} is 1. The contribution from the additional diagrams generated from the expansion of the gauge link is essential to ensure $F_1^p(0)=1$. In other words, the local gauge invariance guarantees charge conservation. Though for the choices of Λ, our results are a little smaller than the empirical values, they are much better than that with dimensional regularization, especially at large Q^2.

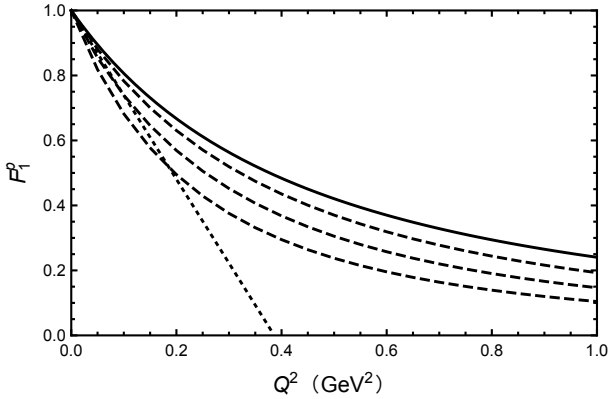

Fig. 2. The Dirac form factor of the proton F_1^p versus momentum transfer Q^2. The three dashed lines, from bottom to top, are for the results with Λ=0.7 GeV, 0.8 GeV and 0.9 GeV, respectively. The solid and dotted lines are for the empirical and dimensional regularization result [18] respectively.

The result of $F_2^p(Q^2)$ is plotted in Fig. 3. The solid, dashed and dotted lines have the same meaning as in Fig. 2, but are for F_2^p. Again, our results are much better than that with dimensional regularization. The empirical lines is within our obtained range of $F_2^p(Q^2)$. From these two figures for the proton form factors, one can see

that the size effect of the nucleon at tree level is very important to get a reasonable result at relatively large Q^2.

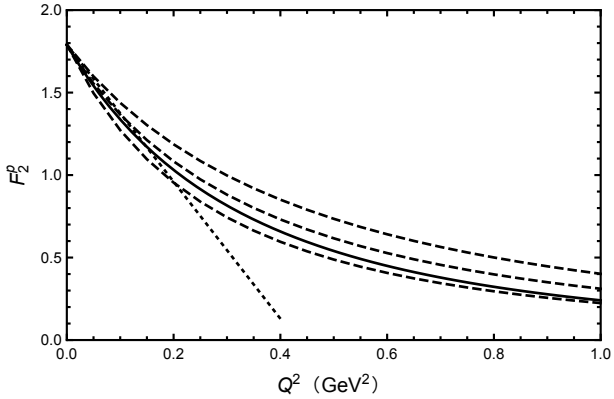

Fig. 3. The Pauli form factor of the proton F_2^p versus momentum transfer Q^2. The three dashed lines, from bottom to top, are for the results with Λ=0.7 GeV, 0.8 GeV and 0.9 GeV, respectively. The solid and dotted lines are for the empirical and dimensional regularization result [18] respectively.

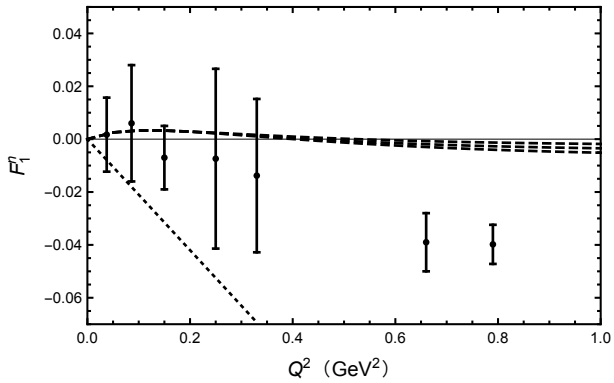

Fig. 4. The Dirac form factor of the neutron F_1^n versus momentum transfer Q^2. The three dashed lines are for the results with Λ=0.7 GeV, 0.8 GeV and 0.9 GeV, respectively. The dotted line is for the dimensional regularization result [18]. The dots with error bars are experimental data [44].

Next we will show the results for the neutron. When we calculate F_1^n and F_2^n, the parameters are chosen to be the same as in the proton case. The results of F_1^n versus Q^2 are shown in Fig. 4. The experimental data with error bars are from Ref. [44]. The sum of all the diagrams in Fig. 1 automatically gives neutron charge 0 at zero momentum transfer. The dashed curves correspond to the three Λs, which are close to each other. All of them are much better than the result with dimensional regularization and comparable with the experimental data.

The curves of F_2^n are plotted in Fig. 5. The empirical values are reproduced very well up to 1 GeV^2 with the proper choice of Λ. In the dimensional regularization, all the calculated proton and neutron form factors are almost linearly dependent on the momentum transfer. It can only describe the form factors at very small Q^2. Numerical calculation shows the loop contribution from K and η mesons is about one order of magnitude smaller than that from the π meson. The major difference of the loop contribution from the chiral perturbation theory calculation is due to the different regularization scheme as applied to the pion loops. Another important difference is that the nonlocal Lagrangian generates both the regulator and momentum dependence of the form factors at tree level, which is quite different from that in pure chiral perturbation theory.

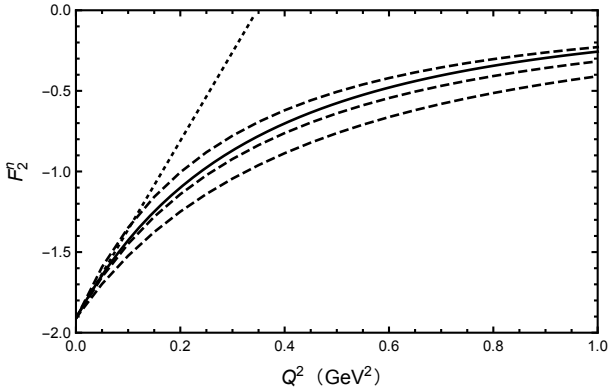

Fig. 5. The Pauli form factor of the neutron F_2^n versus momentum transfer Q^2. The three dashed lines, from top to bottom, are for the results with Λ=0.7 GeV, 0.8 GeV and 0.9 GeV, respectively. The solid and dotted lines are for the empirical and dimensional regularization result [18] respectively.

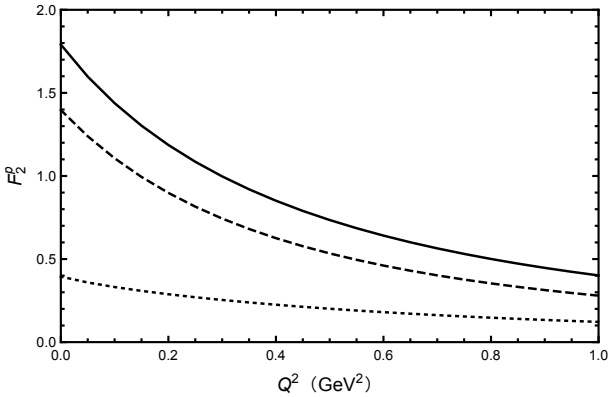

Fig. 6. The Pauli form factor of the proton F_2^p versus momentum transfer Q^2 with Λ 0.9 GeV. The dashed, dotted and solid lines are for the tree level, loop and total contributions respectively.

To see clearly how important the tree level contribution to the form factors is, we show the proton Pauli form factor in Fig. 6 as an example. The dashed, dotted and solid lines are for the tree level, loop and total

contributions to F_2^p respectively. From the figure, the nonlinear Q^2 dependence at tree level is crucial to get a reasonable form factor. The loop contribution gives less curvature. At Q^2=0, the loop contributes 0.4, while the 3-quark core contributes 1.4 to F_2^p. The importance of the nonlinear Q^2 dependence at tree level is similar for the other form factors except for F_1^n, where the tree level contribution is zero. To save space, instead of showing the momentum dependence of the other form factors with figures, we list the results in the table. In Table 1, we list the separate tree and loop contribution to the form factors as well as the total contribution at different momentum transfers. From the table, the tree level contribution is always dominant. Similar to F_2^p, the momentum dependence of F_1^p and F_2^n at tree level is crucial to get a final reasonable Q^2 dependence. The loop contribution provides less curvature in these cases. Our calculation shows that the size effect is very important to get a correct description of the nucleon form factors. The nonlocal Lagrangian generates the momentum dependence of the form factors at tree level. It also generates the regulator for the loop integral. Both of these reflect the non-pointlike nature of the hadrons. Therefore, the regulator makes the loop integral convergent. It also makes the calculated form factors close to the empirical data up to relatively large Q^2.

We should mention that in our calculation, only one free parameter in the dipole regulator is used. The parameters c_1 and c_2 are fixed by experimental F_2^p and F_2^n as in the dimensional regularization. However in the dimensional regularization, besides c_1 and c_2, the lines in the above figures are obtained by four other additional parameters (low energy constants) in order to get the correct electromagnetic radii of the proton and neutron. In our calculation, besides c_1 and c_2, only one parameter in the dipole regulator is used. With this one free parameter, we can get reasonable form factors up to 1 GeV^2. The charge and magnetic radii are calculated instead of fitted, and are comparable with the experimental data. The parameters and the calculated moments and radii are listed in Table 2.

Table 1. The separate tree, loop and total contribution to the nucleon form factors for different Q^2 with Λ=0.9 GeV.

Q^2/GeV^2	F_1^p			F_2^p			F_1^n			F_2^n		
	tree	loop	total	tree	loop	total	tree	loop	total	tree	loop	total
0	0.658	0.342	1	1.4	0.39	1.79	0	0	0	−1.52	−0.39	−1.91
0.25	0.384	0.187	0.571	0.815	0.27	1.085	0	0.00222	0.00222	−0.887	−0.254	−1.141
0.5	0.251	0.119	0.37	0.534	0.201	0.735	0	-0.00126	-0.00126	−0.581	−0.182	−0.763
0.75	0.177	0.083	0.26	0.376	0.155	0.531	0	-0.0037	-0.0037	−0.409	−0.137	−0.546
1	0.132	0.061	0.193	0.28	0.121	0.401	0	-0.00511	-0.00511	−0.304	−0.105	−0.409

Table 2. The parameters and obtained moments and radii for three choices of Λ. The experimental values are listed in the last row.

Λ/GeV	Z	c_1	c_2	F_2^p	F_2^n	r_{Mp}/fm	r_{Ep}/fm	r_{Mn}/fm	r_{En}^2 /fm^2
0.7	0.77	3.29	1.05	1.79	−1.91	0.960	1.052	0.956	−0.145
0.8	0.71	3.37	1.03	1.79	−1.91	0.846	0.941	0.846	−0.146
0.9	0.66	3.46	0.97	1.79	−1.91	0.760	0.856	0.764	−0.149
EXP.	-	-	-	1.79	−1.91	0.836	0.847	0.889	−0.113

5 Summary

We have constructed a nonlocal chiral effective Lagrangian which makes it possible to apply the successful finite-range-regularization to the relativistic case. Different from FRR in the non-relativistic case, here the regulator is not added by hand. It is derived from the nonlocal Lagrangian. The local gauge invariance is regained by the gauge link. As a result, the Dirac form factor of the proton (neutron) at $Q^2 = 0$ is automatically 1 (0) when we study the nucleon form factors with this nonlocal chiral Lagrangian. In this chiral effective model calculation, baryon octet and decuplet intermediate states are included in the one-loop calculation. Comparing with the calculation in dimensional regularization, besides c_1 and c_2, we have only one parameter instead of four parameters in the case of dimensional regularization. With fewer parameters, our results for both proton and neutron are much better, especially at large Q^2. The parameter Λ is found to be 0.8±0.1 GeV, which will give reasonable form factors for both proton and neutron up to $Q^2 = 1$ GeV^2. The calculated charge and magnetic radii are all comparable with the experimental data.

References

1 D.-H. Lu, A. W. Thomas, and A. G. Williams Phys. Rev. C, **57**: 2628–2637 (1998)
2 K. Berger, R. F. Wagenbrunn, and W. Plessas Phys. Rev. D, **70**: 094027 (2004)
3 B. Julia-Diaz, D. O. Riska, and F. Coester Phys. Rev. C, **69**: 035212 (2004)
4 A. J. Buchmann and R. F. Lebed Phys. Rev. D, **67**: 016002 (2003)
5 S. Cheedket, V. E. Lyubovitskij, T. Gutsche, A. Faessler, K. Pumsa-ard, and Y. Yan Eur. Phys. J. A, **20**: 317–327 (2004)
6 R. A. Williams and C. Puckett-Truman Phys. Rev. C, **53**: 1580–1588 (1996)
7 P.-N. Shen, Y.-B. Dong, Z.-Y. Zhang, Y.-W. Yu, and T. S. H. Lee Phys. Rev. C, **55**: 2024–2029 (1997)
8 R. Jakob, P. Kroll, M. Schurmann, and W. Schweiger Z. Phys. A, **347**: 109–116 (1993)
9 G. Hellstern and C. Weiss Phys. Lett. B, **351**: 64–69 (1995)
10 J. M. Zanotti, D. B. Leinweber, A. G. Williams, and J. B. Zhang Nucl. Phys. Proc. Suppl., **129**: 287–289 (2004)
11 S. Boinepalli, D. B. Leinweber, A. G. Williams, J. M. Zanotti, and J. B. Zhang Phys. Rev. D, **74**: 093005 (2006)
12 C. Alexandrou, G. Koutsou, J. W. Negele, and A. Tsapalis Phys. Rev. D, **74**: 034508 (2006)
13 **QCDSF** Collaboration, M. Gockeler, T. R. Hemmert, R. Horsley, D. Pleiter, P. E. L. Rakow, A. Schafer, and G. Schierholz Phys. Rev. D, **71**: 034508 (2005)
14 M. Gockeler et al (QCDSF/UKQCD Collaboration), PoS, **LAT2007**: 161 (2007)
15 **LHPC** Collaboration, R. G. Edwards, G. T. Fleming, P. Hagler, J. W. Negele, K. Orginos, A. V. Pochinsky, D. B. Renner, D. G. Richards, and W. Schroers, PoS, **LAT2005**: 056 (2006)
16 **Lattice Hadron** Collaboration, C. Alexandrou et al, J. Phys. Conf. Ser., **16**: 174–178 (2005)
17 S. J. Puglia, M. J. Ramsey-Musolf, and S.-L. Zhu Phys. Rev. D, **63**: 034014 (2001)
18 T. Fuchs, J. Gegelia, and S. Scherer J. Phys. G, **30**: 1407–1426 (2004)
19 B. Kubis and U. G. Meissner Eur. Phys. J. C, **18**: 747–756 (2001)
20 B. Kubis and U.-G. Meissner Nucl. Phys. A, **679**: 698–734 (2001)
21 R. D. Young, D. B. Leinweber, and A. W. Thomas Prog. Part. Nucl. Phys., **50**: 399–417 (2003)
22 D. B. Leinweber, A. W. Thomas, and R. D. Young Phys. Rev. Lett., **92**: 242002 (2004)
23 P. Wang, D. B. Leinweber, A. W. Thomas, and R. D. Young Phys. Rev. D, **75**: 073012 (2007)
24 P. Wang and A. W. Thomas Phys. Rev. D, **81**: 114015 (2010)
25 C. R. Allton, W. Armour, D. B. Leinweber, A. W. Thomas, and R. D. Young Phys. Lett. B, **628**: 125–130 (2005)
26 W. Armour, C. R. Allton, D. B. Leinweber, A. W. Thomas, and R. D. Young Nucl. Phys. A, **840**: 97–119 (2010)
27 J. M. M. Hall, D. B. Leinweber, and R. D. Young Phys. Rev. D, **88**(1): 014504 (2013)
28 D. B. Leinweber, S. Boinepalli, I. C. Cloet, A. W. Thomas, A. G. Williams, R. D. Young, J. M. Zanotti, and J. B. Zhang Phys. Rev. Lett., **94**: 212001 (2005)
29 P. Wang, D. B. Leinweber, A. W. Thomas, and R. D. Young Phys. Rev. C, **79**: 065202 (2009)
30 P. Wang, D. B. Leinweber, A. W. Thomas, and R. D. Young Phys. Rev. D, **86**: 094038 (2012)
31 P. Wang, D. B. Leinweber, and A. W. Thomas Phys. Rev. D, **89**(3): 033008 (2014)
32 J. M. M. Hall, D. B. Leinweber, and R. D. Young Phys. Rev. D, **89**(5): 054511 (2014)
33 P. Wang, D. B. Leinweber, and A. W. Thomas Phys. Rev. D, **92**(3): 034508 (2015)
34 H. Li, P. Wang, D. B. Leinweber, and A. W. Thomas Phys. Rev. C, **93**(4): 045203 (2016)
35 P. Wang, D. B. Leinweber, A. W. Thomas, and R. D. Young Phys. Rev. D, **79**: 094001 (2009)
36 E. E. Jenkins Nucl. Phys. B, **368**: 190–203 (1992)
37 E. E. Jenkins, M. E. Luke, A. V. Manohar, and M. J. Savage Phys. Lett. B, **302** 482–490 (1993)
38 S. Scherer Adv. Nucl. Phys., **27**: 277 (2003)
39 L. S. Geng, J. Martin Camalich, and M. J. Vicente Vacas Phys. Rev. D, **80**: 034027 (2009)
40 A. Hiller Blin, T. Gutsche, T. Ledwig, and V. E. Lyubovitskij Phys. Rev. D, **92**(9): 096004 (2015)
41 D. B. Leinweber, A. W. Thomas, K. Tsushima, and S. V. Wright Phys. Rev. D, **61**: 074502 (2000)
42 J. Terning Phys. Rev. D, **44**(3): 887–897 (1991)
43 P. Wang Can. J. Phys., **92**: 25–30 (2014)
44 M. Seimetz (A1 Collaboration), Nucl. Phys. A, **755**: 253–256 (2005)